Evaluating 6G Candidate Waveforms for Radar Applications in Joint Communication and Sensing

Bruno S. Pompeo, Marcello L.R. de Campos, José A. Apolinário Jr., and Leandro G. F. Pralon

***Abstract*— In recent years, systems such as digital audio broadcasting and digital video broadcasting, which typically use orthogonal frequency division multiplexing (OFDM) waveforms, have gained prominence within the scientific community as illuminators of opportunity in passive radar systems. However, with the advent of beyond fifth-generation and sixth-generation communication technologies, the limitations of OFDM, particularly its intolerance to high-mobility scenarios, have become apparent. Concurrently, the Joint Communication and Sensing concept, which integrates radar operations with communication systems, has evolved into a viable reality. Hence, other waveforms are emerging as alternatives to OFDM. Orthogonal Time-Frequency Space and Orthogonal Chirp-Division Multiplexing are recent candidates. While most studies focus on communication performance, it is equally important to analyze the performance of these waveforms from the radar perspective, which is often overlooked. In this context, this work carries out a detailed analysis and comparison of radar performance metrics such as range resolution, peak sidelobe levels, integrated sidelobe levels, and Doppler tolerance using traditional radar receiver processors with the emerging waveforms as transmitted signal.**

***Keywords*— JCS, OFDM, OTFS, OCDM, matched filter**

I. Introduction

Joint Communication and Sensing (JCS) is an innovative approach that integrates communication and sensing functionalities into a single unified framework, enhancing the use of electromagnetic spectrum and hardware resources [1]. JCS enables devices to simultaneously communicate and sense their environment, leading to improved network efficiency, enhanced situational awareness, and the potential for new applications in areas such as autonomous driving, smart cities, and Internet of Things (IoT) ecosystems [2], [3].

In recent years, various communication signals have been analyzed and proposed as effective transmit sources for passive radar applications. Several works have identified Digital Audio Broadcast (DAB) and Digital Video Broadcast (DVB) as viable alternatives for both communication and radar applications [4]. The modulation scheme employed in both DAB and DVB is the Orthogonal Frequency Division Multiplex (OFDM). OFDM optimizes the spectrum utilization, offers greater resistance to frequency-selective fading than single-carrier systems, simplifies channel equalization and eliminates inter-symbol interference (ISI) through the use of a cyclic prefix (CP). On the other hand, it introduces a high peak-to-average power ratio (PAPR), and it is susceptible to carrier frequency offset, resulting in degraded performance in high-mobility scenarios [5].

Emerging wireless communication technologies, referred to as beyond 5G (B5G) and 6G technologies need to support high mobility scenarios and massive Multiple-Input Multiple-Output (MIMO) systems, requiring high bandwidth and, consequently, higher carrier frequencies. These spectral characteristics create an environment conducive to high-resolution tracking and location, essential for radar applications, but they also lead to greater Doppler shift and significant free-space attenuation. Therefore, a crucial aspect of the physical layer architecture in B5G/6G systems is the selection of the transmitted waveform [6]. Whereas 4G and 5G cellular networks utilize OFDM at gigahertz frequencies, B5G and 6G demand even higher frequencies to accommodate increasingly dynamic mobility scenarios. However, OFDM faces challenges in this context due to its inherent limitations.

Several studies have proposed alternative waveforms to overcome OFDM limitations [6]–[9]. The evolution of communication systems, including the rise of JCS systems [10], highlights the importance of selecting suitable waveforms for the next stages of B5G and 6G [6], [7]. Candidate waveforms should enhance orthogonality tolerance, reduce sidelobe levels, lower the PAPR value, and offer robustness against channel time and frequency selectivity. In this work, we analyze two such waveforms that show particular promise for radar applications: Orthogonal Chirp-Division Multiplexing (OCDM) [9] and Orthogonal Time Frequency Space (OTFS) [8].

In radar theory, analyzing the performance of a given transmit waveform must include investigating how it can affect target detection, measurement accuracy, resolution, and ambiguities [11]. In the present work, such features are examined within a radar system employing a matched filter architecture. Presumed Doppler shifts caused by the target velocity are also considered to evaluate the Doppler tolerance of the waveforms.

Within this context, our contributions in this work are: 1) investigation and comparison of side lobe level, range resolution and Doppler tolerance for OFDM, OTFS, and OCDM waveforms; and 2) evaluation of the behavior of these waveforms in a matched filter processing radar within the context of a JCS application. The remainder of this paper is organized into five sections. Sections II.A to II.C detail the modulation structures of OFDM, OCDM, and OTFS, respectively. Section III describes the matched filter receiver used in traditional radar systems and discusses important metrics

Bruno S. Pompeo, Federal University of Rio de Janeiro, Rio de Janeiro-RJ, e-mail: pompeo@coppe.ufrj.br; Marcello L.R. de Campos, Electrical Engineering Program, Federal University of Rio de Janeiro, Rio de Janeiro-RJ, e-mail: campos@smt.ufrj.br; José A. Apolinário Jr, Department of Electrical Engineering, Military Institute of Engineering, Rio de Janeiro-RJ, e-mail: apolin@ime.eb.br; Leandro G. F. Pralon, Radar Group, Brazilian Army Technological Center, Rio de janeiro-RJ, e-mail: pralon.leandro@eb.mil.br.
This work was partially supported by FAPERJ contract E-26/210.157/2023.

associated with the matched filter output. Section IV examines the performance of each waveform, comparing them in terms of range resolution, peak-sidelobe ratio (PSLR), integrated-sidelobe ratio (ISLR), and Doppler shift tolerance through a numerical example and simulations. Finally, the conclusions are presented in Section V.

II. Candidate waveforms for JCS

A variety of waveforms have been proposed for next-generation wireless communication systems, particularly within the context of JCS applications. This work covers three candidates: the widely-used OFDM and the promising OCDM and OTFS for radar applications. [12], [13].

Modulated data symbols for transmission are generated using 2^{α}-QAM modulation, $\alpha \in \mathbb{N}$, from a serial bit-stream. We assume that these modulated data symbols are distributed into predefined frames with NM samples. Each data vector $\mathbf{x} \in \mathbb{C}^{NM\times 1}$ is allocated in an $N \times M$ matrix. From this moment, the modulation scheme differs for each waveform and more details are presented in the following.

A. OFDM Modulation

In recent years, OFDM has emerged as a widely adopted modulation technique in various communication systems. It finds extensive application in commercial sectors, including wireless communication systems, DVB-T and DAB systems, and 4G LTE cellular systems [14]. It is a multicarrier waveform with orthogonal subcarriers generally windowed by a rectangular pulse shape that results in a sinc function in the frequency domain.

Considering M OFDM symbols composed each by N modulated data symbol, the data matrix is given by

$$\mathbf{X} = \begin{pmatrix} x_0 & x_N & \cdots & x_{(M-1)N} \\ x_1 & x_{N+1} & \cdots & x_{(M-1)N+1} \\ \vdots & \vdots & \ddots & \vdots \\ x_{N-1} & x_{2N-1} & \cdots & x_{MN-1} \end{pmatrix},$$

i.e., $\mathbf{X} = \text{vec}^{-1}(\mathbf{x})$[1]. The data matrix, to be transmitted, is multiplied by matrix $\mathbf{F}_{\text{N}}$, the $N \times N$ IDFT matrix[2]. This operation is responsible to allocate each modulated data symbol in a subcarrier. A CP, consisting of the last N_{CP} elements of each column in $\mathbf{F}_{\text{N}}\mathbf{X}$, is inserted in each OFDM symbol:

$$\mathbf{S}_{\text{CP-OFDM}} = \mathbf{C}\mathbf{F}_{\text{N}}\mathbf{X}, \tag{1}$$

where

$$\mathbf{C} = \begin{pmatrix} \mathbf{0}_{N_{\text{CP}}\times N-N_{\text{CP}}} & \mathbf{I}_{N_{\text{CP}}} \\ & \mathbf{I}_N \end{pmatrix}$$

is an $N_T \times N$ matrix that adds the CP samples, with $N_T = N + N_{\text{CP}}$, and $\mathbf{S}_{\text{CP-OFDM}}$ the transmission data matrix. In this way, each symbol with CP has N_T samples and the transmission signal in discrete time, after the Parallel-to-Serial (P/S) conversion, is given by $\text{s}_{\text{CP-OFDM}} = \text{vec}(\mathbf{S}_{\text{CP-OFDM}})$.

Communication systems that utilize the OFDM modulation have their own transmission structure composed of guard interval, pilots, and transport parameter signalling (TPS). It is beyond the scope of this work to consider such characteristics.

B. OCDM Modulation

OCDM is a modulation technique based on the discrete Fresnel transform (DFnT), proposed in [9]. OCDM has emerged as a potential alternative to OFDM, attributed to its enhanced resilience to multipath propagation [13]. OCDM integrates the principles of OFDM with *chirp* signaling to enhance performance in challenging communication environments. Essentially, the modulated data symbols are distributed across orthogonal *chirps* rather than orthogonal sinusoids.

A *chirp* is a modulated frequency signal in which the frequency increases (up-chirp) or decreases (down-chirp) linearly with time. In pulsed radar systems, *chirps* are popular due to their effectiveness in pulse compression and robustness against Doppler effects [11].

The corresponding OCDM discrete time domain version is derived from an inverse discrete Fresnel transform (IDFnT) applied in the data matrix $\mathbf{X}$, and given by [9]

$$\mathbf{S}_{\text{OCDM}} = \frac{1}{\sqrt{N}}\mathbf{\Phi}_{\text{N}}^{\text{H}}\mathbf{X}, \tag{2}$$

with $\mathbf{\Phi}_{\text{N}} \in \mathbb{C}^{N\times N}$ having its elements given by

$$\Phi(n,k) = \text{e}^{-\text{j}\frac{\pi}{4}} \begin{cases} \text{e}^{\text{j}\frac{\pi}{N}(n-k)^2}, & N \text{ even;} \\ \text{e}^{\text{j}\frac{\pi}{N}\left(n-k+\frac{1}{2}\right)^2}, & N \text{ odd,} \end{cases} \tag{3}$$

with $^{\text{H}}$ being the Hermitian operator.

In order to show that the integration of the OCDM transmitter (and receiver) into the existing OFDM system is possible, notice that the IDFnT transform consists of the IDFT transform with additional quadratic phases [9]. Eq. (2) can be rewritten as

$$\mathbf{S}_{\text{OCDM}} = \frac{1}{\sqrt{N}}\mathbf{\Theta}_1^{\text{H}}\mathbf{F}_{\text{N}}\mathbf{\Theta}_2^{\text{H}}\mathbf{X}, \tag{4}$$

where $\mathbf{\Theta}_1$ and $\mathbf{\Theta}_2$ are $N \times N$ diagonal matrices whose elements are given by

$$\mathbf{\Theta}_1(n) = \text{e}^{\text{-j}\frac{\pi}{4}} \begin{cases} \text{e}^{\text{j}\frac{\pi}{N}n^2}, & N \text{ even;} \\ \text{e}^{\text{j}\left(\frac{\pi}{4N}+\frac{\pi}{N}(n^2+n)\right)}, & N \text{ odd,} \end{cases}$$

$$\mathbf{\Theta}_2(n) = \begin{cases} e^{\text{j}\frac{\pi}{N}n^2}, & N \text{ even;} \\ e^{\text{j}\frac{\pi}{N}(n^2-n)}, & N \text{ odd,} \end{cases}$$

with $0 \leq n \leq N-1$. Similarly to the OFDM symbols, where the IDFT synthesizes the data symbols in orthogonal sinusoids, the synthesis of a bank of discretized modulated chirp waveforms can be realized by the IDFnT. The CP is applied to each $\mathbf{S}_{\text{OCDM}}$ column and then after P/S operation the signal is transmitted.

[1]Let vec(.) be the operation (linear transformation) which converts a matrix into a single column vector, concatenating the columns of the original matrix. We define $\text{vec}^{-1}(.)$ as the operation that converts a single column vector into a matrix of appropriate dimensions.

[2]Matrix $\mathbf{F}_{\text{N}}$ is the inverse discrete Fourier transform (IDFT), an $N \times N$ matrix which coefficients are $\frac{1}{\sqrt{N}}\exp(\text{j}2\pi nm/N)$, with n the row index and m the column index.

C. OTFS Modulation

The OTFS scheme, unlike other waveforms, maps data from the Delay-Doppler (DD) domain rather than the well-known Time-Frequency (TF) domain. Data can be converted directly to the TF domain through a linear transformation called Inverse Symplectic Finite Fourier Transform (ISSFT) [8].

Consider $\mathbf{X}$ as the data matrix now in the DD domain. The corresponding data matrix in the TF domain, $\mathbf{X}_{\text{TF}}$, is written as

$$\mathbf{X}_{\text{TF}} = \mathbf{F}_{\text{N}}^{\text{H}} \mathbf{X} \mathbf{F}_{\text{M}}, \tag{5}$$

where $\mathbf{F}_{\text{M}}$ is the $M \times M$ IDFT matrix. The left multiplication by $\mathbf{F}_{\text{N}}^{\text{H}}$ and the right multiplication by $\mathbf{F}_{\text{M}}$ constitute the ISFFT transformation.

Similar to the OFDM modulation, the symbols in (5) are transmitted after undergoing an IDFT transformation, generating the following matrix:

$$\mathbf{S}_{\text{OTFS}} = \mathbf{F}_{\text{N}} \mathbf{X}_{\text{TF}} = \mathbf{X} \mathbf{F}_{\text{M}}. \tag{6}$$

Subsequently, N_{CP} samples corresponding to the CP are added to each column of the $\mathbf{S}_{\text{OTFS}}$ matrix using matrix $\mathbf{C}$. After the serialization of the columns, the signal is transmitted.

Fig. 1 summarizes the block diagram of the transmission chain corresponding to the waveforms investigated herein.

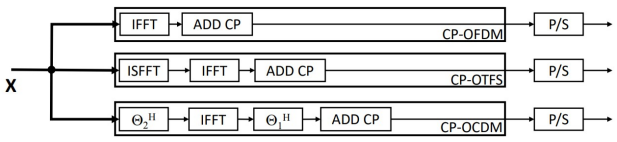

Fig. 1
BLOCK DIAGRAM ILLUSTRATING THE TRANSMITTER FOR EACH CANDIDATE WAVEFORM.

III. MATCHED FILTER RECEIVER

Modern radar systems employ sophisticated methods to detect target reflection signals in an environment and estimate their kinematic characteristics. The matched filter forms the basis for the receiver design of the radar signal processor [11]. By correlating the received signal in discrete time ($\mathbf{r}$) with the conjugated replica of the transmitted signal in discrete time ($\mathbf{s}$), the matched filter is used to maximize the signal-to-noise ratio (SNR) at the output of the radar receiver [11], and is defined as

$$f(\tau) = \sum_{k=-\infty}^{\infty} s^*[k-\tau] r[k]. \tag{7}$$

Fig. 2 shows the basic architecture of transmission and reception chains in a JCS system, without additional processing such as coding or equalization. The multipath delay-Doppler channel $h(\tau, \nu)$ can be express as

$$h(\tau, \nu) = \sum_{i=1}^{P} h_i \delta(\tau - \tau_i) \delta(\nu - \nu_i), \tag{8}$$

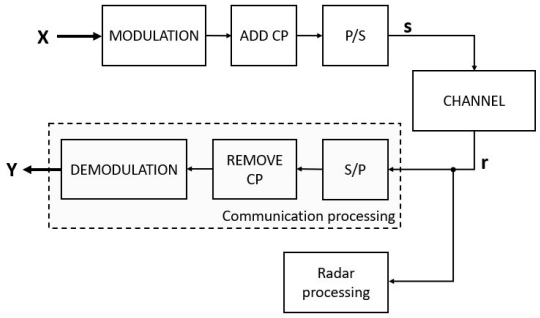

Fig. 2
BASIC ARCHITECTURE OF TRANSMISSION AND RECEPTION IN A JCS SYSTEMS.

where h_i denotes the complex gain of the i-th reflector, $\delta(.)$ denotes the Dirac delta function and τ and ν are delay and Doppler shift variables, respectively.

In this work, we compute the matched filter considering two distinct inputs: 1) the vector of transmitted signal ($\mathbf{s}$) and the vector of received signal ($\mathbf{r}$), commonly used in only-radar application [11]; 2) the vector of transmitted data (vec($\mathbf{X}$)) and the vector of demodulated data (vec($\mathbf{Y}$)) proposed in radar-communication application [12].

From the output of the matched filter, it is possible to evaluate relevant metrics to radar systems, such as range resolution, PSLR, and ISLR. These metrics are detailed in the following.

A. Range resolution

Range resolution (ΔR) in radar systems is a fundamental concept that determines how well a radar system can distinguish between two or more targets that are close to each other in distance. The range resolution gives the minimum distance between two objects at which the radar can still identify them as separate entities. The relation between range resolution and transmitted signal features is given by

$$\Delta R = k_r \frac{c}{2B},$$

with c the speed light, B the bandwidth of the signal, and k_r a constant greater or equal to one that depends basically on pulse shaping, filtering, or windowing. The range resolution can be estimated as the width of the main lobe of the matched filter output. The criterion commonly used is the half-power (or -3 dB) point, where the magnitude of $|f(\tau)|$ falls to half its maximum value. The narrower the main lobe, the better the range resolution.

B. PSLR

PSLR is a measure related to the behavior of sidelobes in matched filtering output. It represents the largest sidelobe to the mainlobe peak and indicates the capability of detecting weak reflections in the presence of high reflections. PSLR is described as [15]

$$\text{PSLR} = 10\log\left(\frac{\max\{|f(\tau')|^2\}}{\max\{|f(\tau)|^2\}}\right),$$

where $\max\{|f(\tau)|^2\}$ is the global squared magnitude maximum of $f(\tau)$ and $\max\{|f(\tau')|^2\}$ is the value of the largest sidelobe. When the PSLR is high (value closer to zero), the peak sidelobe levels are closer to the mainlobe peak, which can mask weak targets. Conversely, when the PSLR is low, the peak sidelobe levels are much lower than the mainlobe peak, allowing for the detection of weak targets.

C. ISLR

ISLR indicates the proportion of energy contained within the sidelobes in relation to the energy within the mainlobe. In other words, the ISLR measures how much energy is leaking from the mainlobe; it is described as [15]

$$\text{ISLR} = 10\log\left(\frac{\sum_{\tau=-\infty}^{\tau_{\max}-\tau_0}|f(\tau)|^2 + \sum_{\tau=\tau_{\max}+\tau_0}^{\infty}|f(\tau)|^2}{\sum_{\tau=\tau_{\max}-\tau_0}^{\tau_{\max}+\tau_0}|f(\tau)|^2}\right).$$

A lower ISL is generally preferred as it indicates a cleaner signal with less potential for interference from sidelobe emissions.

IV. Numerical Example

In this section, we discuss the performance of the candidate waveform OFDM, OTFS, and OCDM in radar applications. This analysis takes into account the ΔR, PSLR, ISLR, and also a Doppler tolerance evaluation given through the compression loss (the ratio between the maximum value in the matched filter output and the maximum value in the matched filter output considering zero Doppler shift). In terms of communication metrics, we present the PAPR achieved in each waveform.

PAPR provides the fluctuation level in a signal by comparing its peak power to its average power. A high PAPR indicates significant signal peaks, which impact the efficiency of power amplifiers. Higher PAPR leads to lower efficiency in RF power amplifiers. PAPR is typically expressed in decibels (dB) and is calculated as:

$$\text{PAPR} = 10\log\left(\frac{\max(|s[k]|^2)}{\text{mean}(|s[k]|^2)}\right),$$

where $\max(|s[k]|^2)$ refers to the maximum value of the squared magnitude of the elements of the discrete-time signal s, and $\text{mean}(|s[k]|^2)$ is the average of the squared magnitude of the elements of the discrete-time signal $\mathbf{s}$.

We present a numerical example using B5G or 6G communication settings compatible with those used in [12], as summarized in Table I. Our simulations are conducted under noiseless and zero-delay conditions. The results focus on comparing the matched filter responses of OFDM, OTFS, and OCDM waveforms, as well as evaluating the PAPR findings.

For a fair comparison, we assume the bandwidth of each *chirp* equal to 10% of the OFDM bandwidth. Hence, the bandwidths in the three modulations are approximately the same, as shown in the Fig. 3. Note that the OCDM spectrum decays quicker than OFDM and OTFS.

TABLE I

Simulation Parameters

Parameter	Value
Carrier Frequency (f_C)	24 GHz
Number of subcarriers (N)	256
CP length (N_{CP})	32
Signal bandwidth (B)	10 MHz
Subcarrier spacing ($\Delta f = \frac{B}{N}$)	39.0625 kHz
Number of symbols (M)	4

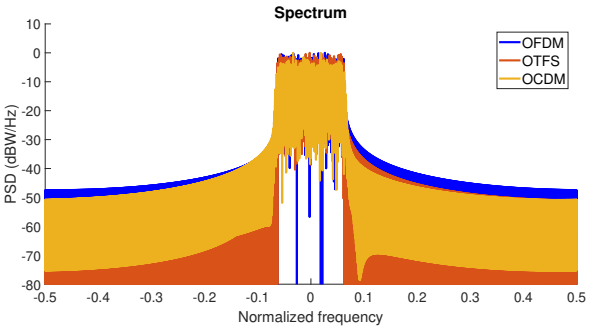

Fig. 3

Spectrum of OFDM, OTFS and OCDM waveforms.

The PAPR analysis is evaluated as the probability of the PAPR of the signal exceeding a predetermined value PAPR_0. In Fig. 4, the PAPR is provided in the three waveforms, considering $N = 256$. OTFS has been shown to have the best PAPR. OCDM presents performance similar to that of OFDM.

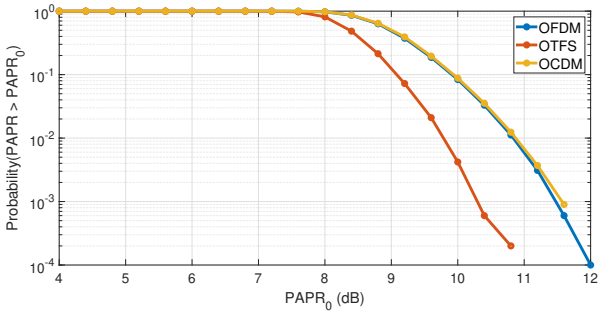

Fig. 4

PAPR performance of 6G candidate waveforms.

The results for metrics PSLR and ISLR as functions of the Doppler shift are presented in Fig. 5. The range resolution remains nearly constant with increasing Doppler shift independently of the waveform, with $k_r \approx 1.21$ (see Section III.A); therefore, the corresponding curves have been omitted. Compression losses are presented in Fig. 6, where the left side illustrates the result in the context of the matched filter processing as discussed in [11] and the right side illustrates the result in the context of the matched filter processing as

discussed in [12] (see Section III).

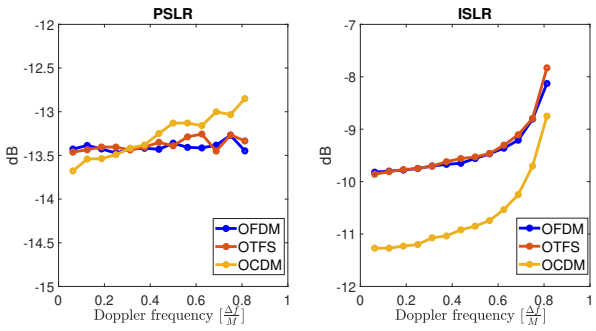

Fig. 5

PSLR AND ISLR AS A FUNCTION OF THE DOPPLER SHIFT.

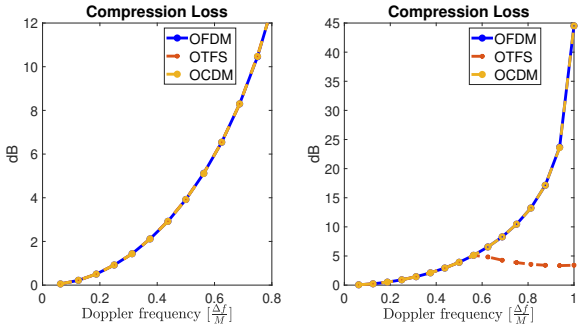

Fig. 6

COMPRESSION LOSS AS A FUNCTION OF THE DOPPLER SHIFT HAVING $(\mathbf{r})$ AND $(\mathbf{s})$ (LEFT) AND VEC$(\mathbf{X})$ AND VEC$(\mathbf{Y})$ (RIGHT) AS INPUTS.

Fig. 5, on the left, shows that there is no significant change in PSLR with an increase in Doppler shift, and all waveforms behave in the same way. Furthermore, on the right, it shows that the OCDM waveform demonstrates a significantly lower ISLR compared to the other two waveforms with the increase in Doppler shift. Compression loss curves for OFDM, OTFS and OCDM increase exponentially when the matched filter processing uses vectors $\mathbf{s}$ and $\mathbf{r}$ as inputs. In the case where matched filter processing uses vec$(\mathbf{X})$ and vec$(\mathbf{Y})$ as inputs, the curves for OFDM and OCDM increase exponentially in the same manner as the previous matched filter processing, but the curve for OTFS reaches a maximum value of approximately 5 dB and then decreases. This result is attributed to fractional Doppler shifts[3].

V. CONCLUSIONS

This paper investigates candidate waveforms for JCS systems, specifically focusing on OFDM, OCDM, and OTFS modulations. Our study concentrated on radar-related metrics, particularly those derived from the output of a matched filter.

[3]Fractional Doppler is caused by insufficient sampling in the Doppler domain. In other words, it happens when the Doppler shift is equal to $\frac{\kappa}{MT}$, with $\kappa \in \left(-\frac{1}{2}, \frac{1}{2}\right)$ and T is the symbol duration in seconds [16].

The PAPR of the OTFS modulation was found to be inferior to those of OCDM and OFDM, with the latter two exhibiting very similar PAPR values. This indicates that OTFS may offer significant advantages in terms of power efficiency and signal robustness, which are critical factors in the performance of communication and radar systems.

Our findings indicate that the PSLR of all three waveforms remains largely unaffected by Doppler shift, exhibiting similar values. Conversely, the ISLR increases with rising Doppler shift; however, OCDM has a significantly lower ISLR compared to the other two waveforms. Using the matched filter with transmitted and received signal vectors, the compression losses are consistent across all waveforms and escalate exponentially with increasing Doppler shift. In contrast, using the transmitted and demodulated data vectors, OTFS shows remarkable resilience to Doppler shift, unlike OFDM and OCDM. These results highlight the potential of the OTFS modulation for maintaining performance in high-mobility scenarios, making it a promising candidate for future JCS systems.

REFERENCES

[1] R. Thomä, T. Dallmann, S. Jovanoska, P. Knott, and A. Schmeink, "Joint communication and radar sensing: An overview," in *15th European Conference on Antennas and Propagation (EuCAP)*. IEEE, 2021.
[2] A. Ericsson, "Joint communication and sensing in 6G networks," 2021.
[3] Z. Feng, Z. Wei, X. Chen, H. Yang, Q. Zhang, and P. Zhang, "Joint communication, sensing, and computation enabled 6G intelligent machine system," *IEEE Network*, vol. 35, no. 6, 2021.
[4] D. Poullin, "Passive detection using digital broadcasters (DAB, DVB) with COFDM modulation," *IEE Proceedings-Radar, Sonar and Navigation*, vol. 152, no. 3, 2005.
[5] S. Kumara and S. Deshwala, "A Review on Orthogonal Time Frequency Space Modulation," in *Workshop on Computer Networks & Communications. IEEE*, 2021.
[6] F. Conceição, M. Gomes, V. Silva, R. Dinis, A. Silva, and D. Castanheira, "A survey of candidate waveforms for beyond 5G systems," *Electronics*, vol. 10, no. 1, 2020.
[7] B. A. Adoum, K. Zoukalne, M. S. Idriss, A. M. Ali, A. Moungache, and M. Y. Khayal, "A Comprehensive Survey of Candidate Waveforms for 5G, beyond 5G and 6G Wireless Communication Systems," *Open Journal of Applied Sciences*, vol. 13, no. 1, 2023.
[8] R. Hadani, S. Rakib, M. Tsatsanis, A. Monk, A. J. Goldsmith, A. F. Molisch, and R. Calderbank, "Orthogonal time frequency space modulation," in *IEEE Wireless Communications and Networking Conference*, 2017.
[9] X. Ouyang and J. Zhao, "Orthogonal Chirp Division Multiplexing," *IEEE Transactions on Communications*, vol. 64, no. 9, 2016.
[10] S. D. Liyanaarachchi, T. Riihonen, C. B. Barneto, and M. Valkama, "Optimized waveforms for 5G–6G communication with sensing: Theory, simulations and experiments," *IEEE Transactions on Wireless Communications*, vol. 20, no. 12, 2021.
[11] M. I. Skolnik, *Introduction to Radar systems*, 3rd ed. McGraw-Hill New York, 2001.
[12] P. Raviteja, K. T. Phan, Y. Hong, and E. Viterbo, "Orthogonal Time Frequency Space (OTFS) modulation based radar system," in *2019 IEEE Radar Conference (RadarConf)*, 2019.
[13] L. G. de Oliveira, M. B. Alabd, B. Nuss, and T. Zwick, "An OCDM radar-communication system," in *14th IEEE European Conference on Antennas and Propagation*, 2020.
[14] T. Hwang, C. Yang, G. Wu, S. Li, and G. Y. Li, "OFDM and its wireless applications: A survey," *IEEE Transactions on Vehicular Technology*, vol. 58, no. 4, 2008.
[15] S. Dayarathna, P. Smith, R. Senanayake, and J. E. Member, "OTFS based Joint Radar and Communication: Signal Analysis using the Ambiguity Function," *IEEE Signal Processing Letters*, vol. 31, 2024.
[16] D. Shi, W. Wang, L. You, X. Song, Y. Hong, X. Gao, and G. Fettweis, "Deterministic pilot design and channel estimation for downlink massive MIMO-OTFS systems in presence of the fractional Doppler," *IEEE Transactions on Wireless Communications*, vol. 20, no. 11, 2021.